HEFAT2012
9th International Conference on Heat Transfer, Fluid Mechanics and Thermodynamics
16-18 July 2012
Malta

BIFURCATION OF INTERNALLY HEATED FLOW IN A VERTICAL PIPE

Senoo T., Deguchi K. and Nagata M.*
*Author for correspondence
Department of Aeronautics and Astronautics,
Graduate School of Engineering,
Kyoto University,
Kyoto, 606-8501,
Japan
E-mail: nagata@kuaero.kyoto-u.ac.jp

ABSTRACT

The development of fluid motion in an infinitely long circular pipe with homogeneously distributed internal heat source is examined numerically. The pipe is placed vertically in the gravity field with the pipe wall temperature being kept constant. The motion of the fluid is driven upward by the buoyancy force as well as downward by an applied pressure gradient along the pipe axis. Thus, the basic velocity profile can become inflectional and we may anticipate that the flow may become unstable in contrast to the isothermal pipe flow which is known to be linearly stable for any Reynolds number.

We find that the linear instabilities always occur within the region where the basic velocity profile is inflectional but not totally reverse. Our nonlinear analysis indicates that there are two types of nonlinear solutions, referred to as $spirals$ and $ribbons$. They bifurcate simultaneously from the same point on the neutral curve. Furthermore, the branch of the ribbon extends far inside the region where the basic state is linearly stable and reaches the isothermal limit, creating a nonlinear solution in 'pure' pipe flow for the case with $Pr = 0$. For the case with $Pr = 7$ nonlinear interactions between spirals with different azimuthal wavenumbers are observed.

INTRODUCTION

To evaluate heat and mass transfer for flow in a pipe is one of the vital factors in designing a chemical plant and a nuclear power plant. Yet, it is only a decade ago that even an isothermal case saw some progress. Until then, the problem of transition from laminar flow with a parabolic velocity profile to turbulence in a pipe, started by Reynolds in 1883, had been remained unsolved. The difficulty to solve the problem rests in the fact that the isothermal pipe flow is linearly stable for any Reynolds number and so the transition from laminar flow to turbulent flow must occur abruptly. Since the linear critical points are absent, weakly nonlinear analysis does not work and nonlinear solutions must be sought directly. Some clue for nonlinear pipe flows did exist in the study for plane Couette flow [1], another canonical flow without linear critical points: nonlinear solutions in plane Couette flow were discovered, therein, for the first time by making the flow unstable by introducing a spanwise system rotation, following the bifurcating solution branch and switching off the rotation to find a survived nonlinear solution. The survived solution at the zero rotation is characterized by quasi-streamwise vortices, streamwise streaks and a distorted inflectional mean flow. The observation of the flow structure of the nonlinear solution in plane Couette flow led to the so-called self-sustaining process, SSP, for turbulent flow [2].

By introducing an artificial force which would constitute the SSP, nonlinear solutions in a pipe were obtained [3,4]. The nonlinear solution, now called *exact coherent structure*, ECS, which is a saddle point in the phase space possessing both stable and unstable manifolds. Turbulent flow in a pipe is believed to be represented by trajectory wondering around the ECS's in the phase space [5].

In the present paper we make the flow linearly unstable by distributing an internal heat source homogeneously inside a vertical pipe. Our system is, therefore, physically realizable in contrast to the previous studies [3,4]. The basic velocity profile can become inflectional due to the upward buoyancy force, measured by the Grashof number, Gr, in the presence of an applied axially downward pressure drop, measured by the Reynolds number, Re.

First, we identify a region in the (Re, Gr)-space where the basic flow is unstable by a linear stability analysis. It is found that linear instabilities occur within the region in the (Re, Gr)-space where the basic velocity profile is inflectional and partially reverse.

Our nonlinear analysis reveals that there are two types of nonlinear solutions, spirals and ribbons, bifurcating from the

same neutral points. Spirals are characterized by a vortical structure which are tilted in one way with respect to the pipe axis, whereas ribbons have a double vortical structure tilted with an equal angle in both ways.

Furthermore, for the vanishing Prandtl number, we are able to detect a path in the (Re, Gr)-space leading to the isothermal pipe flow solution, starting from a ribbon solution in the thermal case.

For the finite Prandtl number interactions between spirals with various azimuthal wavenumbers are observed.

NOMENCLATURE

a	[-]	Radius (non-dimensional)
a^*	[m]	Radius (dimensional)
g^*	[m/s^2]	Gravitational acceleration
q	[-]	Internal heat source intensity (non-dimensional)
q^*	[K/s]	Internal heat source intensity (dimensional)
Gr	[-]	Grashof number
m	[-]	Azimuthal wavenumber
Pr	[-]	Prandtl number
Re	[-]	Reynolds number
T	[-]	Mean temperature
$\boldsymbol{U}$	[-]	Velocity
$\check{V}$	[-]	Mean aximuthal velocity
$\check{W}$	[-]	Mean axial velocity
ξ_i	[-]	Cylindrical coordiates: (r, θ, z)
t	[-]	Time
$\boldsymbol{u}$	[-]	Total velocity
$\hat{\boldsymbol{u}}$	[-]	Velocity disturbance

Special characters

β	[-]	Axial wavenumber
γ^*	[1/K]	Volume expansion coefficient
κ^*	[m^2/s]	Thermal diffusivity
ν^*	[m^2/s]	Kinematic viscosity
Π	[-]	Pressure
σ	[-]	Growth rate
ϑ	[-]	Total temperature
$\hat{\vartheta}$	[-]	Temperature disturbance

Subscripts

B	[-]	Basic state
b	[-]	Bulk quantity

MATHEMATICAL FORMULATION

We consider an incompressible fluid motion inside an infinitely long circular pipe with the radius, a, placed vertically in the gravity field. The temperature of the pipe wall is kept constant while internal heat sources with an intensity, q, are homogeneously distributed inside the pipe. The motion of the fluid is driven by the buoyancy force as well as the pressure gradient applied downward along the pipe (see Fig.1).

Applying the Boussinesq approximation and taking a_*, a_*^2/ν_*, $\nu_*^2/(\gamma_* g_* a_*^3)$, respectively, as the length, time and temperature scales, where ν_* is the kinematic viscosity, γ_* is the volume expansion coefficient and g_* is the acceleration due to gravity, we obtain the non-dimensional basic equations in a cylindrical coordinate system, (r, θ, z), with the unit vectors, $(\boldsymbol{e}_r, \boldsymbol{e}_\theta, \boldsymbol{e}_z)$:

the equation of continuity:

$$\nabla \cdot \boldsymbol{u} = 0, \tag{1}$$

the momentum equation:

$$\frac{D\boldsymbol{u}}{Dt} = -\frac{\partial \Pi}{\partial \xi_i} + \vartheta \boldsymbol{k} + \nabla^2 \boldsymbol{u}, \tag{2}$$

the temperature equation:

$$Pr \frac{D\vartheta}{Dt} = \nabla^2 \vartheta + 2Gr. \tag{3}$$

where $\boldsymbol{u}$ is the fluid velocity, Π is the pressure and ϑ is the temperature. The no-slip condition and the constant temperature condition are imposed on the pipe wall at $r = 1$:

$$\boldsymbol{u}(1,\ t) = 0, \qquad \vartheta(1,\ t) = 0. \tag{4}$$

The Reynolds number, Re, and the Grashof number, Gr, control the development of the flow in the system. Pr is the Prandtl number which is prescribed by the material property of the fluid:

$$Re = \frac{W_{0*} a_*}{\nu_*}, \quad Gr = \frac{g_* \gamma_* q_* a_*^5}{2\nu_*^2 \kappa_*}, \quad Pr = \frac{\nu_*}{\kappa_*}, \tag{5}$$

where W_{0*} is the central velocity when $Gr = 0$ and κ_* is the coefficient of thermal diffusivity.

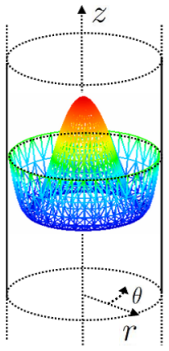

Fig. 1: The model.

BASIC STATE

The laminar basic steady state, W_B, T_B, can be easily obtained from equations (2) and (3) by assuming its functional dependency only on r:

$$W_B(r) = Re(1 - r^2) + \frac{1}{32} Gr(1 - r^2)(3 - r^2), \tag{6}$$

$$T_B(r) = \frac{1}{2} Gr(1 - r^2). \tag{7}$$

When the internal heat source is absent, $Gr = 0$, the basic steady flow has a well known parabolic velocity profile directing vertically downwards. As Gr is increased the central

part gets hotter and a reverse upward flow starts developing. The basic steady flow can be classified in the (Re, Gr)-space in terms of the existence of inflection points and reverse flow components as shown in Fig.2.

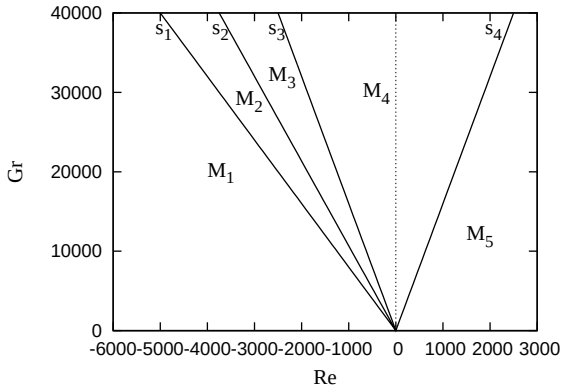

Fig. 2: The classification of the basic flow in the (Re, Gr)-plane.

In the figure, no inflection points exist in the profile of $W_B(r)$ in the regions indicated by M_1 and M_5 and two inflection points exists in M_2, M_3 and M_4. $W_B(r)$ possesses a reversal component at $r = 0$ in M_2 and M_3. The flow is totally reversed in M_4 and M_5. Typical profiles in each region are shown in Fig.3

DISTURBANCE EQUATIONS

We superimpose disturbances, ($\hat{\boldsymbol{u}}$, $\hat{\vartheta}$, $\hat{\Pi}$), on the basic state, ($\boldsymbol{U}_B, T_B.\ \Pi_B$). Disturbances are assumed to be periodic in the axial direction. For convenience, $\hat{\boldsymbol{u}}$, $\hat{\vartheta}$ are separated into mean parts, $\check{\boldsymbol{U}} = (0, \check{V}, \check{W})$, $\check{T}$ and residuals $\breve{\boldsymbol{u}}$, $\breve{\vartheta}$:

$$\boldsymbol{u} = \boldsymbol{U}_B + \check{V}\boldsymbol{j} + \check{W}\boldsymbol{k} + \breve{\boldsymbol{u}}, \tag{8}$$

$$\vartheta = T_B + \check{T} + \breve{\vartheta}, \tag{9}$$

$$\Pi = \Pi_B + \hat{\Pi}. \tag{10}$$

Substitution of these disturbances into equations (1), (2) and (3) leads to the equations for disturbances.

$$\nabla \cdot \breve{\boldsymbol{u}} = 0, \tag{11}$$

$$\frac{\partial \breve{\boldsymbol{u}}}{\partial t} + \quad (\hat{\boldsymbol{U}} \cdot \nabla)\breve{\boldsymbol{u}} + (\breve{\boldsymbol{u}} \cdot \nabla)\hat{\boldsymbol{U}} + (\breve{\boldsymbol{u}} \cdot \nabla)\breve{\boldsymbol{u}} = -\nabla\breve{\Pi} + \breve{\vartheta}\boldsymbol{k} + \triangle\breve{\boldsymbol{u}}, \tag{12}$$

$$\overline{(\breve{\boldsymbol{u}} \cdot \nabla)v + \frac{\breve{u}\breve{v}}{r}} + \check{V}'' + \frac{1}{r}\check{V}' - \frac{1}{r^2}\check{V} = \partial_t \check{V} \tag{13}$$

$$\overline{(\breve{\boldsymbol{u}} \cdot \nabla)w} + \check{W}'' + \frac{1}{r}\check{W}' + \check{T} = \partial_t \check{W} \tag{14}$$

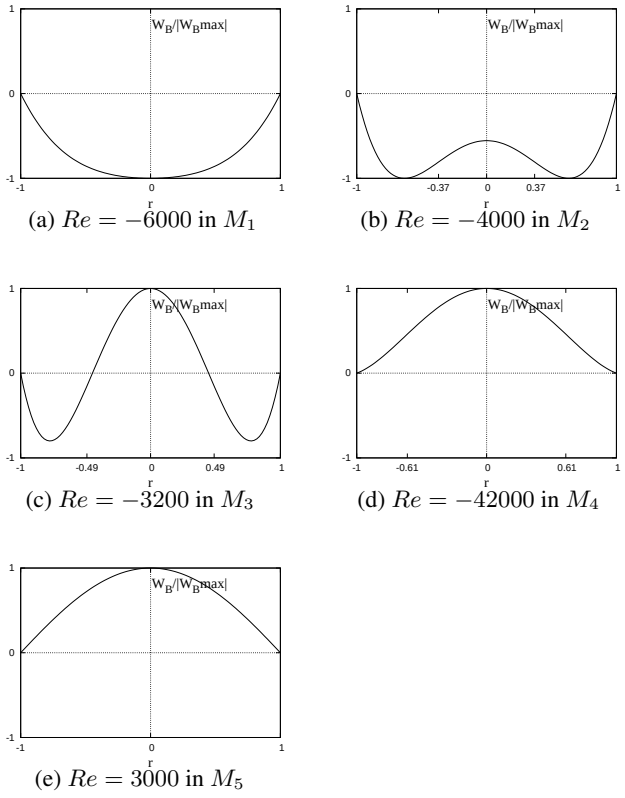

(a) $Re = -6000$ in M_1 (b) $Re = -4000$ in M_2

(c) $Re = -3200$ in M_3 (d) $Re = -42000$ in M_4

(e) $Re = 3000$ in M_5

Fig. 3: The basic velocity profiles, $W_B(r)$, along $Gr = 40000$.

$$\frac{\partial \breve{\vartheta}}{\partial t} + \quad (\hat{\boldsymbol{U}} \cdot \nabla)\breve{\vartheta} + (\breve{\boldsymbol{u}} \cdot \nabla)\hat{T} + (\breve{\boldsymbol{u}} \cdot \nabla)\breve{\vartheta} = \tfrac{1}{Pr}\triangle\breve{\vartheta}, \tag{15}$$

$$Pr\overline{(\breve{\boldsymbol{u}} \cdot \nabla)\breve{\vartheta}} + (\check{T}'' + \frac{1}{r}\check{T}') = Pr\partial_t\check{T}, \tag{16}$$

where $\hat{\boldsymbol{U}} = \boldsymbol{U}_B + \check{\boldsymbol{U}}$ and $\hat{T} = T_B + \check{T}$.

LINEAR STABILITY ANALYSIS

We omit the nonlinear terms with respect to disturbances in equations (12) and (15). Also, we disregard equations (13), (14) and (16) for the mean flow components because they are created by the quadratic interactions of the residual parts. The residual part of the velocity disturbance, $\breve{\boldsymbol{u}}$, is separated into a poloidal part, $\nabla \times \nabla \times (r\phi\boldsymbol{e}_r)$, and a toroidal part, $\nabla \times (r\psi\boldsymbol{e}_r)$:

$$\breve{\boldsymbol{u}} = \nabla \times \nabla \times (r\phi\boldsymbol{e}) + \nabla \times (r\psi\boldsymbol{e}). \tag{17}$$

Note that the above representation satisfies equation (11) automatically.

We assume periodicity in the θ- and z-direction with the wavenumber pair (m, β) and expand disturbances by the modified Chebyshev polynomials, $T_l(r)$, in the r-direction,

$$(\phi, \psi, \vartheta) = \sum_0^L (a_\ell, b_\ell, c_\ell)\exp[im\theta + i\beta z + \sigma t]T_\ell(r), \tag{18}$$

where σ is the growth rate. Then, we evaluate the resultant disturbance equations at the collocation points defined by

$$r_i = \cos\Big(\frac{i\,\pi}{2(L+2)}\Big),\ (i = 1, \ldots, L+1), \tag{19}$$

where L is the highest order of the modified Chebyshev polynomials used. Then, the problem becomes

$$\boldsymbol{A}\boldsymbol{x} = \sigma \boldsymbol{B}\boldsymbol{x} \tag{20}$$

with σ as the eigenvalue. Here, matrices $\boldsymbol{A}$ and $\boldsymbol{B}$ are functions of Re, Gr, Pr, m and β, and the elements of the vector $\boldsymbol{x}$ stand for the amplitude a_ℓ, b_ℓ, c_ℓ of the disturbance components.

The neutral curves, where the real part of σ vanishes, are calculated for the azimuthal wavenumbers, $m = 0, 1, 2, 3$ (see Fig.4). The basic state is unstable inside the wedged region in each figure. The axial wavenumber, β, varies along the curves. It would be interesting to see that the unstable regions are always confined within M_2 and M_3, where the basic velocity profile is inflectional but not totally reverse. It should be noted that the purely hydrodynamic flow, $Pr = 0$, can be unstable only for $m = 1$ (we should add that the stability has been examined up to $Gr = 100000$).

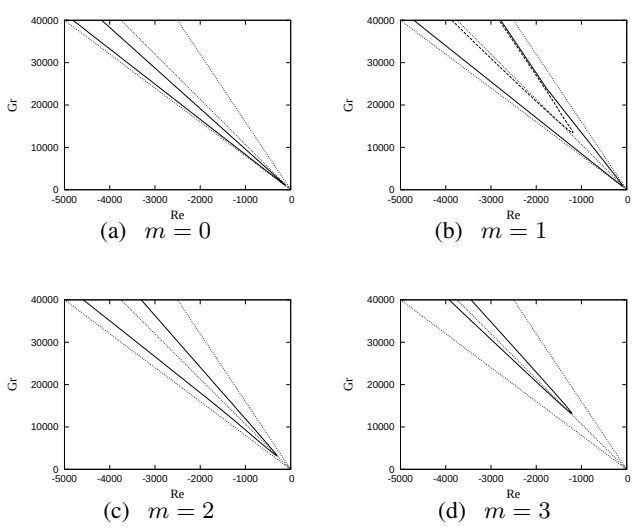

(a) $m = 0$ (b) $m = 1$ (c) $m = 2$ (d) $m = 3$

Fig. 4: The neutral curves for $Pr = 0$ (dashed curve) and $Pr = 7$ (solid curve). The optimal value of β is taken along the curves. Note that instabilities for $Pr = 0$ can be seen only in (b).

NONLINEAR ANALYSIS

The residual part of the velocity disturbance is expressed by a poloidal part, $\nabla \times \nabla \times (r\phi \boldsymbol{e}_r)$, and a toroidal part, $\nabla \times (r\psi \boldsymbol{e}_r)$, as in the linear analysis:

$$\check{\boldsymbol{u}} = \nabla \times \nabla \times (r\phi \boldsymbol{e}_r) + \nabla \times (r\psi \boldsymbol{e}_r). \tag{21}$$

We expand $(\phi, \psi, \check{\vartheta})$ in the z- and θ-directions by the Fourier series with the wavenumber pair (m, β) and expand all the disturbances by the modified Chebyshev polynomials, $T_l(r)$, in the r-direction,

$$(\phi, \psi, \check{\vartheta}) = \sum_{\ell=0}^{L} \sum_{k=-K}^{K} \sum_{n=-N}^{N} (a_{\ell,k,n}, b_{\ell,k,n}, c_{\ell,k,n}) \times \exp[ikm\theta + in\beta(z - ct)] T_\ell(r), \tag{22}$$

and

$$(\check{V}, \check{W}, \check{\Pi}) = \sum_{\ell=0}^{L} (d_\ell, e_\ell, f_\ell) T_\ell(r), \tag{23}$$

where we have assumed that the disturbances travell in the z-direction with the phase speed c.

We evaluate the disturbance equations (12) - (16) at the collocation points (19) to obtain the algebraic equation,

$$A_{ij} x_j + B_{ijk} x_j x_k = 0 \tag{24}$$

where the components of x_i represent the expansion coefficients, $a_{\ell,k,n}$, $b_{\ell,k,n}$, $c_{\ell,k,n}$, $d_{\ell,k,n}$, $e_{\ell,k,n}$ and $f_{\ell,k,n}$ (plus the phase speed, c). The matrices, A_{ij} and B_{ijk}, are determined as a function of Re, Gr, Pr, m and β. Solutions are sought by using Newton=Raphson iterative method.

We choose the bulk Reynolds number as a nonlinear measure:

$$Re_b = \frac{1}{\pi} \int_0^{2\pi} \int_0^1 (W_B(r) + \check{W}(r)) r dr d\theta. \tag{25}$$

RESULTS

We examine two cases, $Pr = 0$ and $Pr = 7$. First, we describe the $Pr = 0$ case. It is found that two types of nonlinear solutions bifurcate from the neutral curve. We call one of them *spiral* and the other *ribbon*. Spirals are characterized by a vortical structure which is tilted in one way with respect to the pipe axis, whereas ribbons have a double vortical structure tilted with the equal angle in both ways (see Fig.5). Fig.6 shows that the spiral and the ribbon with $(m, \beta) = (1, 1.0)$ bifurcate from the same point on the neutral curve. It can be seen that the branch of the spiral exists within the wedged region where the basic state is unstable, simply bridging two neutral points, whereas the branch of the ribbon extends far inside the region where the basic state is stable.

It would be worthwhile examining how far the branch of the ribbon extends for other values of β. In particular, it would be of great interest to see whether the branch can reach the line of the isothermal case, $Gr = 0$. Our successful attempt to find a isothermal solution is described in Fig.7. We start from the neutral point at $(Re, Gr) = (-2869, 30000)$ (open circle) for $\beta = 1.44$ and follow a path by keeping $Gr = 30000$ and increasing Re first up to $(Re, Gr) = (1500, 30000)$ (filled square). We are able to reach the isothermal case $(Re, Gr) = (1500, 0)$ (filled triangle) by decreasing Gr from $(Re, Gr) = (1500, 30000)$.

Having obtained a ribbon at $(Re, Gr) = (1500, 0)$, we now explore the branch of isothermal pipe flow solutions as a function of Re. We find that the branch experiences a turning point at $Re \simeq 1000$ when Re is decreased from 1500. Then the

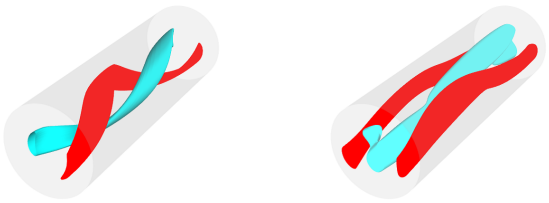

(a) Spiral (b) Ribbon

Fig. 5: Isosurfaces of the streamwise vorticity of spiral (a) and ribbon (b). $(m, \beta) = (1, 1.0)$, $Gr = 30000$.

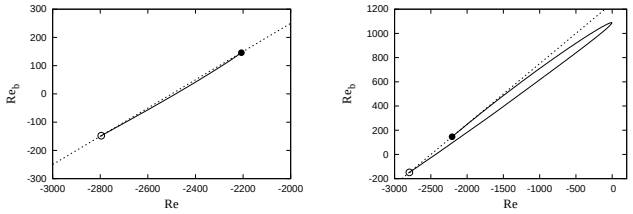

(a) Spiral (b) Ribbon

Fig. 6: Branches of the spiral (a) and the ribbon (b) bifurcating from the same points on the neutral curve. $Pr = 0$. $(m, \beta) = (1, 1.0)$, $Gr = 30000$. Note the difference in scale between (a) and (b).

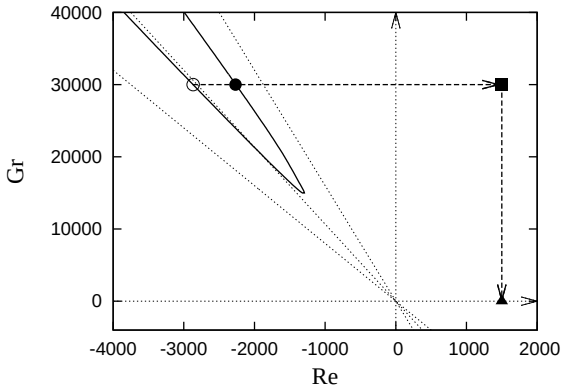

Fig. 7: The path from $(Re, Gr) = (-2869, 30000)$ (open circle) to the isothermal case $(Re, Gr) = (1500, 0)$ (filled triangle) via $(Re, Gr) = (1500, 30000)$ (filled square). $(m, \beta) = (1, 1.44)$.

branch changes direction towards larger Re as shown in Fig.8. Close examination of the solution (see Fig.9) indicates that our isothermal solution is identical to the mirror symmetric travelling waves [6].

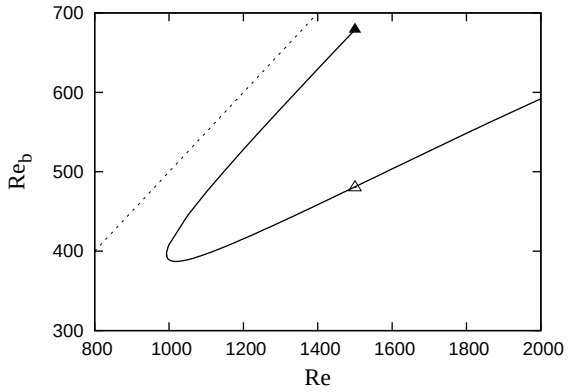

Fig. 8: The bifurcation diagram for isothermal pipe flow, $Gr = 0$. $(m, \beta) = (1, 1.44)$.

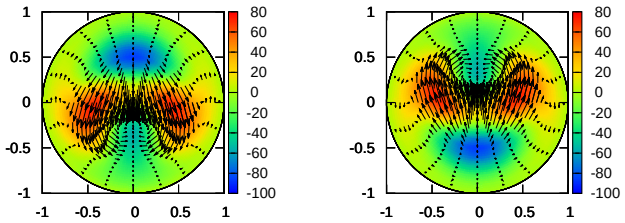

(a) $z = 0$ (b) $z = \pi$

Fig. 9: Cross-sectional flow pattern of the ribbon for isothermal pipe flow on the upper branch at $Re_b = 1200$. (a) $z = 0$. (b) $z = \pi$. $(m, \beta) = (1, 1.0)$.

In the thermal case with $Pr = 7$ unstable regions for $m = 0, 1, 2$ and 3 overlap in the (Re, Gr)-space (see Fig.4) and mode interactions with different m becomes possible as exemplified by Fig.10. In the figure we see that the branches of two spirals with $(m, \beta) = (1, 1.0)$ and $(m, \beta) = (2, 2.0)$, which bifurcate from the neutral points indicated by the filled circles and triangles, respectively, merge at the points indicated by the crosses.

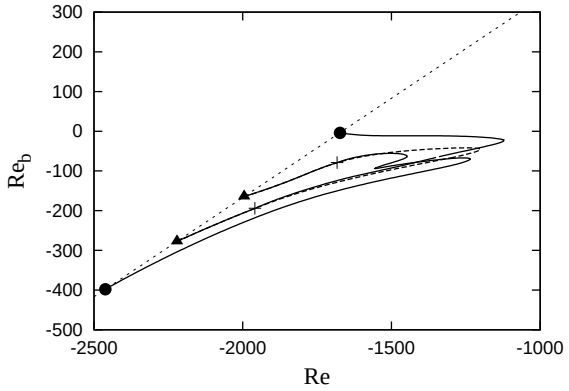

Fig. 10: The mode interaction of spirals with $(m, \beta) = (1, 1.0)$ (dashed curve) and $(m, \beta) = (2, 2.0)$ (solid curve) at $Gr = 20000$ for $Pr = 7$. The dotted straight line represents the laminar flow.

CONCLUSION

The bifurcation of flows of fluid in a pipe driven by the buoyancy force due to a homogeneously distributed internal heat source and an applied pressure drop along the pipe axis is analyzed. The basic state becomes unstable in a parameter region where the basic velocity profile is inflectional. It is found that two types of nonlinear solutions, spirals and ribbons, bifurcate simultaneously from the point on the neutral curve. By following the nonlinear solution branch in the parameter space the isothermal solution in a pipe is recovered for $Pr = 0$. Although our isothermal nonlinear solution of pipe flow is not new, we stress that it is obtained for the first time by considering a physically realizable system, not by introducing an artificial force [3,4]. For $Pr = 7$, nonlinear interactions between spirals with different azimuthal wavenumbers are observed.

REFERENCES

[1] Nagata M., Three-dimensional finite-amplitute solutions in Plane Couette flow : bifurcation from infinity, *Journal of Fluid Mechanics*, Vol. 217, 1990, pp. 519-527

[2] Waleffe F., Three dimensional coherent states in plane shear flows, *Physical Review Letters*, Vol. 19, 1998, pp. 4140-4143

[3] Faisst H., and Eckhardt B., Traveling waves in pipe flow, *Physical Review Letters*, Vol. 91, 2003, 224502-1–4

[4] Wedin H., and Kerswell R R., Exact coherent structures in pipe flow, *Journal of Fluid Mechanics*, Vol. 508, 2004, pp. 333-371

[5] Hof B., van Doorne C W H., Westerweel J., Nieuwstadt F T M., Faisst H., Eckhardt B., Wedin H., Kerswell R R and Waleffe F., Experimental observation of nonlinear travelng waves in turbulent pipe flow, *Science*, Vol. 305, 2004, pp. 1594-1598

[6] Pringle C C and Kerswell R R, Asymmetric, helical and mirror-symmetric travelling waves in pipe flow, *Physical Review Letters*, Vol. 99, 2007, 074502-1–4